Analysis of the Backscatter Spectrum in an Ionospheric Modification Experiment

by

Hongjin Kim

June 1973

SUIPR Report No. 509

Sponsored by

NASA Grant NGL 05-020-176
and
Defense Advanced Research Projects Agency
ARPA Order No. 1733

INSTITUTE FOR PLASMA RESEARCH
STANFORD UNIVERSITY, STANFORD, CALIFORNIA

ANALYSIS OF THE BACKSCATTER SPECTRUM IN AN IONOSPHERIC MODIFICATION EXPERIMENT

by

Hongjin Kim

SUIPR Report No. 509

June 1973

Sponsored by

NASA Grant NGL 05-020-176

and

Defense Advanced Research Projects Agency
(ARPA Order No. 1733; Program Code No. 2E20)
through the Office of Naval Research
(Contract No. N00014-67-A-0112-0066)

Institute for Plasma Research
Stanford University
Stanford, California

CONTENTS

LIST OF FIGURES

ANALYSIS OF THE BACKSCATTER SPECTRUM IN AN IONOSPHERIC MODIFICATION EXPERIMENT

by
Hongjin Kim
Institute for Plasma Research
Stanford University
Stanford, California

ABSTRACT

The purpose of this study is to compare predictions of the backscatter spectrum, including effects of ionospheric inhomogeneity, with experimental observations of incoherent backscatter from an artificially heated region. Our calculations show that the strongest backscatter echo received is not, in fact, from the reflection level, but from a region some distance below (about 0.5 km for an experiment carried out at Arecibo), where the pump wave from a HF transmitter ($\sim$ 100 kW) is below the threshold for parametric amplification. By taking the standing wave pattern of the pump into account properly, the present theory explains the asymmetry of the up-shifted and down-shifted plasma lines in the backscatter spectrum, and the several peaks typically observed in the region of the spectrum near the HF transmitter frequency.

I. INTRODUCTION

From experimental results obtained at Arecibo (Carlson, Gordon and Showen, 1972; Kantor, 1972), it is believed that the enhanced heating and anomalous absorption occurring in the ionosphere are mainly due to parametric decay instabilities; the HF ordinary (pump) wave propagating in the F-layer from a high power transmitter ($\sim$ 100 kW) decays into electron plasma and ion acoustic waves to enhance the plasma fluctuations (DuBois and Goldman, 1965; Nishikawa, 1968). Several analyses have been carried out of the saturation spectra in homogeneous (DuBois and Goldman, 1972a and b; Valeo, Oberman and Perkins, 1972; Kruer and Valeo, 1972; Harker, 1972; Kuo and Fejer, 1972; Fejer and Kuo, 1972; Perkins and Valeo, 1973) or inhomogeneous (Arnush, Fried and Kennel, 1972a and b) plasmas, with the assumption that the pump field is well above the threshold for parametric amplification. This results in saturation of the electron plasma waves due to their nonlinear Landau damping by positive ions, or due to their absorption by electrons whose orbits are nonlinearly perturbed by the waves (Bezzerides and Weinstock, 1972).

However, some essential features of the backscatter spectrum still remain to be explained. For example, Carlson et al. (1972) have obtained a pair of plasma lines in the spectrum enhanced by the pump wave (f_0 = 5.62 MHz). These plasma lines are shifted up and down from the incoherent scatter diagnostic beam (f_i = 430 MHz) by $f_0 - f_a$, where f_a ($\approx$ 4 kHz) is the frequency of the ion acoustic waves generated, and differ from each other in the intensities of the peaks. As shown in Fig. 1, Kantor (1972) has also observed several maxima and minima near the peaks of the spectrum. So far, these features of the spectrum have not been explained.

The purpose of the present analysis is to take the inhomogeneity of the ionosphere into account and to compare our predictions with observations of incoherent scatter. In contrast to most of the previous analyses, our theory assumes that the pump is below the threshold. Section II is concerned with the pump wave. Its intensity is derived as a function of height. In Section III, the intensity of the parametrically enhanced

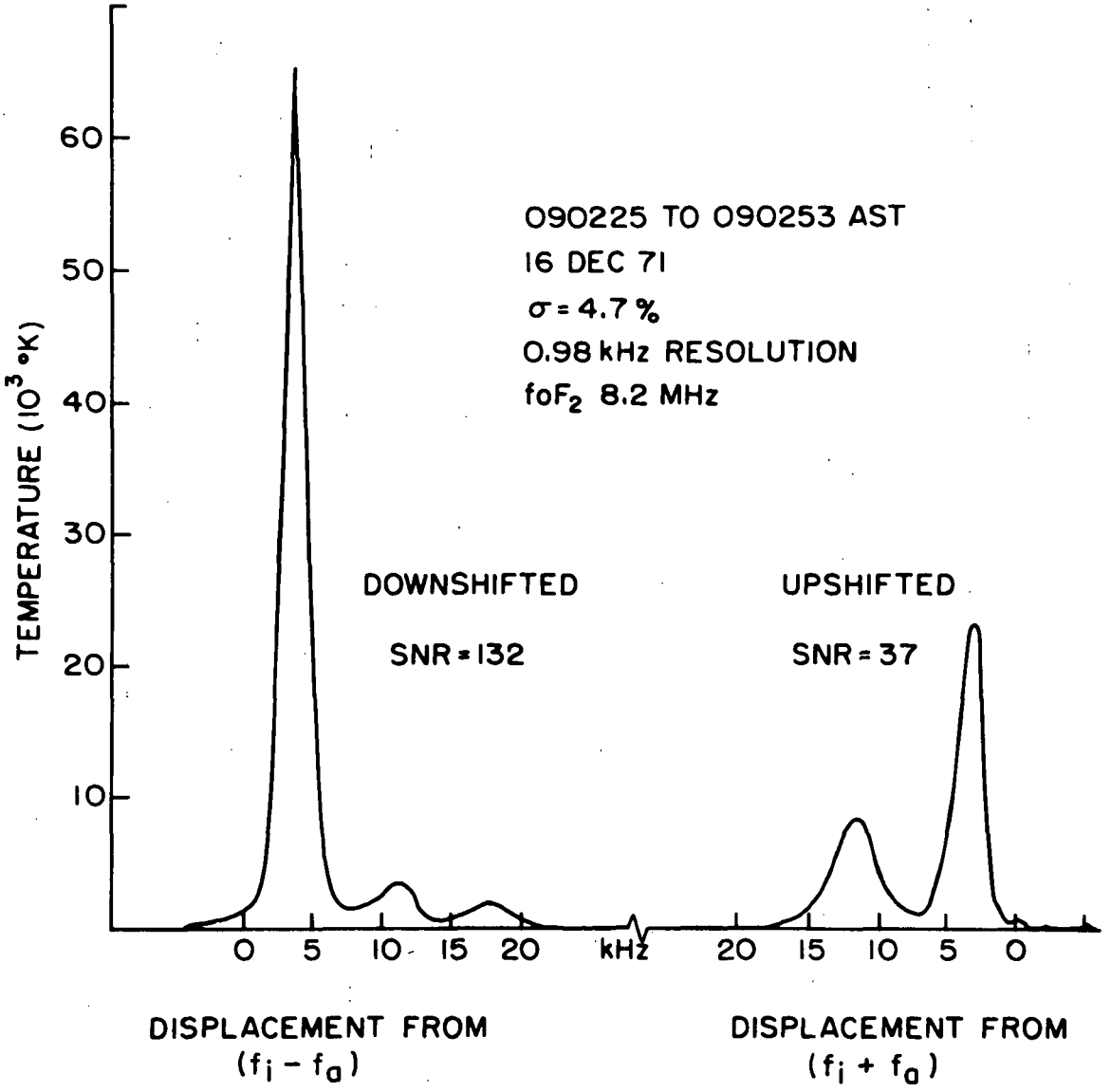

FIG. 1. Frequency spectrum obtained by incoherent backscatter at Arecibo (Kantor, 1972).

electron plasma wave is obtained from the kinetic wave equation. Section IV is devoted to the incoherent scatter experiment performed at Arecibo, and frequency spectra are obtained for several cases. Our assumptions are discussed and predictions are compared to experimental data in Section V.

II. INTENSITY OF THE PUMP WAVE

As the pump wave from the HF transmitter propagates vertically upward in the ionosphere, its group velocity decreases very sharply near, and reaches zero at, the reflection level, as shown in Fig. 2. Since more slowly moving waves spend a longer time in a location, and are thus able to exchange energies more effectively, we shall assume that energy from the pump wave is deposited in the ionosphere only at or very near its reflection level and we neglect the depletion of its intensity due to the linear or nonlinear loss in the region of interest. The present investigation is primarily concerned with heating at frequencies below the penetration frequency, so that the electron density profile can be approximated by a linear profile, as shown in Fig. 2(a). For simplicity, we neglect the geomagnetic field. After the pump field is found, however, it is regarded as being aligned in the direction of the geomagnetic field.

A vertically propagating ordinary wave, of angular frequency ω_0, is described by the wave equations

$$\frac{d^2E}{dz^2} + \left(\frac{\omega_0 h_0}{c}\right)^2 \epsilon(z)E = 0 , \qquad \text{for } z \geq 0 \text{ (in the ionosphere)}$$

$$\frac{d^2E}{dz^2} + \left(\frac{\omega_0 h_0}{c}\right)^2 E = 0 , \qquad \text{for } z < 0 \text{ (in the free space),} \tag{1}$$

where z is the height measured from the base of the ionosphere ($z = 0$), and is normalized to the scale height h_0; c is the speed of light; the wave magnetic field is related to the electric field by

$$B = \frac{1}{i\omega_0 h_0} \frac{dE}{dz} , \tag{2}$$

and the plasma equivalent permittivity, $\epsilon(z)$, is given by

$$\epsilon(z) = 1 - \frac{\omega_p^2}{\omega_0^2} = 1 - z . \tag{3}$$

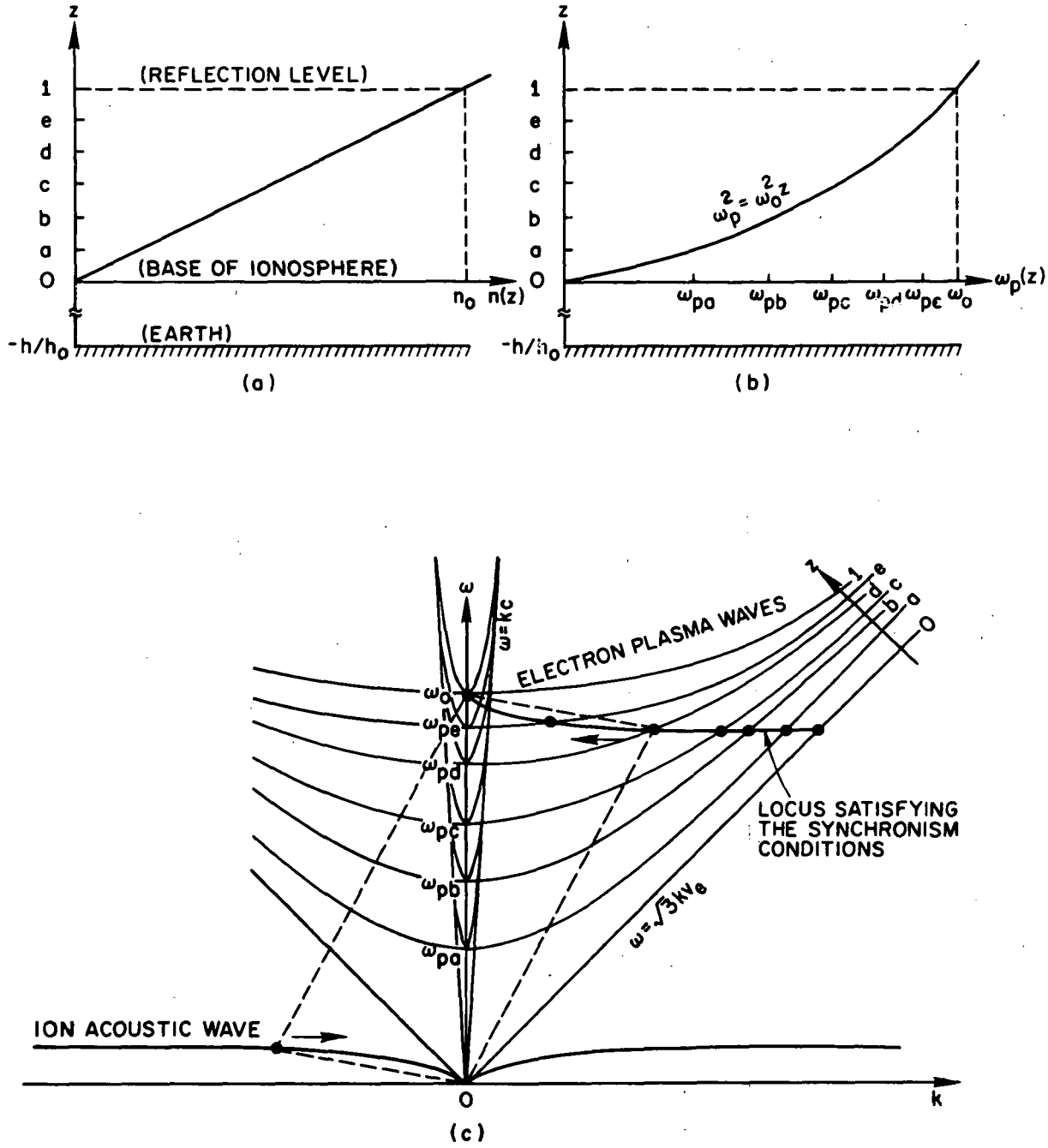

FIG. 2. The electron density and the electron plasma frequency are shown in (a) and (b), respectively, as functions of z. (c) shows the synchronism parallogram for decay instability at different heights in the ionosphere.

The solution to Eq. (1) yields

$$E = a\,Ai(-\zeta) + b\,Bi(-\zeta) , \qquad \text{for } z \geq 0 ,$$

$$E = E_0\left[\exp(-i\zeta_0^{3/2}z) + R\exp(i\zeta_0^{3/2}z)\right], \quad \text{for } z < 0 , \tag{4}$$

where Ai and Bi are the Airy integral functions (Abramowitz and Stegun, 1964); R is the reflection coefficient, and the variables ζ and ζ_0 are defined by

$$\zeta = \zeta_0(1-z) , \quad \zeta_0 = \left(\frac{\omega_0 h_0}{c}\right)^{2/3} . \tag{5}$$

The magnitude of the electric field intensity of the incident pump wave at $z = 0$, E_0, is given by

$$E_0 = \left(60\,\frac{P_0 G}{h^2}\right)^{1/2} \qquad (V/m) , \tag{6}$$

where the average heater power P_0 is in watts; h is the height of the base of the ionosphere from the ground, and the gain, G, of the antenna is given by

$$G = \frac{2\pi A}{c^2}\, f_0^2 , \tag{7}$$

where A is the aperture. In the absence of anomalous absorption, it is customary to put $b = 0$ in (4) because the electric field has to vanish as $z \to \infty$ (Ginzberg, 1964; Budden, 1961). In the present situation, where most of the pump wave energy is deposited at or near the reflection level, however, we assume that the electric field vanishes in $z \geq 1$ due to absorption, and phenomenogically keep the Bi term in the region below the reflection level ($0 \leq z < 1$).

Application of the boundary conditions of continuity of E and B at $z = 0$, and use of (2), reduce (4) to the form

$$|E|^2 = S\,|E_0|^2 , \tag{8}$$

where the swelling factor, S, is given by

$$S = \pi\zeta_0^{1/2}\left|\left\{\exp\left[-i\left(\frac{2}{3}\zeta_0^{3/2} - \frac{\pi}{4}\right)\right] + R\exp\left[i\left(\frac{2}{3}\zeta_0^{3/2} - \frac{\pi}{4}\right)\right]\right\}\mathrm{Ai}(-\zeta)\right.$$
$$\left. + \left\{\exp\left[-i\left(\frac{2}{3}\zeta_0^{3/2} + \frac{\pi}{4}\right)\right] + R\exp\left[i\left(\frac{2}{3}\zeta_0^{3/2} + \frac{\pi}{4}\right)\right]\right\}\mathrm{Bi}(-\zeta)\right|^2 , \tag{9}$$

and use has been made of (Abramowitz and Stegun, 1964)

$$\mathrm{Ai}(x)\mathrm{Bi}'(x) - \mathrm{Ai}'(x)\,\mathrm{Bi}(x) = \frac{1}{\pi} . \tag{10}$$

Noting that $\zeta_0 \gg 1$, use has also been made of the following asymptotic expressions for the Airy integral functions valid for $|x| \gg 1$

$$A_i(-x) \approx \frac{1}{\pi^{1/2}}\,x^{-1/4}\sin\left(\frac{2}{3}x^{3/2} + \frac{\pi}{4}\right) , \quad A_i'(-x) \approx -\frac{1}{\pi^{1/2}}\,x^{1/4}\cos\left(\frac{2}{3}x^{3/2} + \frac{\pi}{4}\right),$$

$$B_i(-x) \approx \frac{1}{\pi^{1/2}}\,x^{-1/4}\cos\left(\frac{2}{3}x^{3/2} + \frac{\pi}{4}\right), \quad B_i'(-x) \approx \frac{1}{\pi^{1/2}}\,x^{1/4}\sin\left(\frac{2}{3}x^{3/2} + \frac{\pi}{4}\right). \tag{11}$$

The familiar results of S and R in the absence of the absorption are recovered from (9) by letting the Bi term equal zero (Ginzberg, 1964; Budden, 1961), as

$$S = 4\pi\zeta_0^{1/2}\,\mathrm{Ai}^2(-\zeta) , \qquad R = \exp\left[-i\left(\frac{4}{3}\zeta_0^{3/2} - \frac{\pi}{2}\right)\right] . \tag{12}$$

At the reflection level ($\zeta = 0$), the swelling factor becomes

$$S = 4\pi c_0^2\zeta_0^{1/2}\left[1 + |R|^2 + 2|R|\cos\left(\frac{4}{3}\zeta_0^{3/2} + \frac{\pi}{6} + \psi\right)\right],$$

$$c_0 \equiv \mathrm{Ai}(0) = 3^{-1/2}\mathrm{Bi}(0) = \frac{3^{-2/3}}{(-1/3)!} , \tag{13}$$

where ψ is the phase of the reflection coefficient, R . The condition that the WKB solution be a good approximation to (1) is $|\zeta| \gg 1$. In this region, (9) becomes

$$S = \left(\frac{\zeta_0}{\zeta}\right)^{1/2}\left\{1 + |R|^2 + 2|R|\cos\left[\frac{4}{3}\left(\zeta_0^{3/2} - \zeta^{3/2}\right)+\psi\right]\right\} . \qquad (14)$$

Figure 2 shows how the swelling factor varies with height for small $|R|$, in the region where the WKB approximation is valid.

The reflection coefficient, R , can be measured from the echo of the pump wave. Hence, the field intensities of the pump wave at the reflection level, and in the region where the WKB approximation is valid, are determined by (8) with the swelling factors given by (13) and (14), respectively.

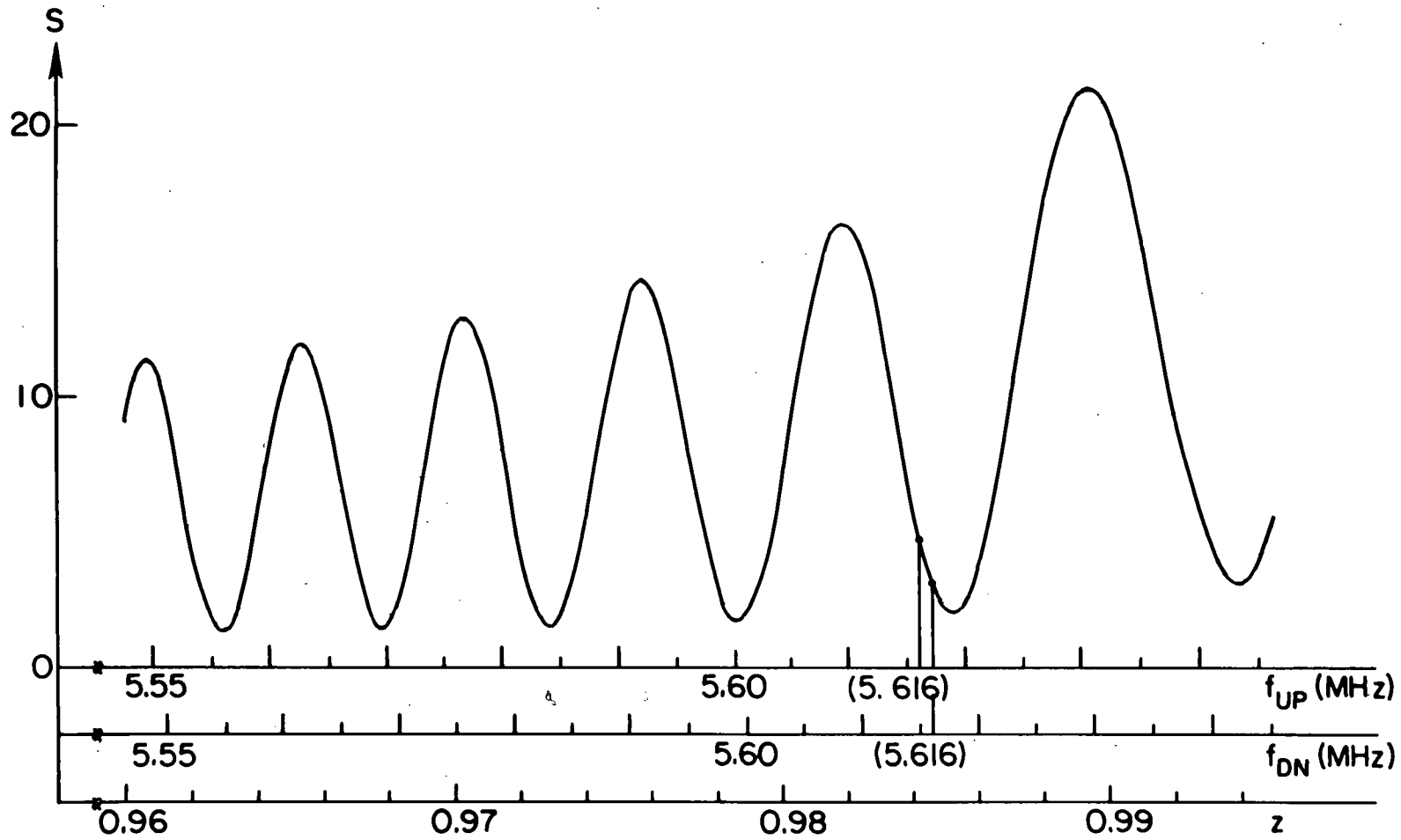

FIG. 3. Swelling factor for $|R| = 1/2$ and $\psi = 0$ as function of z. The frequency scales are obtained from (25).

III. KINETIC WAVE EQUATION FOR THE ENHANCED PLASMA WAVE

Figure 2(c) shows a set of electron plasma wave dispersion waves at different heights ($z = 0$ to 1) and a locus satisfying the synchronism conditions for parametric interaction among the pump wave $(\omega_0, \underset{\sim}{k}_0)$, the electron plasma wave $(\omega, \underset{\sim}{k})$ and the ion acoustic wave $(\omega_a, \underset{\sim}{k}_a)$. As shown in the figure, the electron plasma wave may be excited at any height in the ionosphere. We assume that the pump field is below threshold so that higher order processes such as the nonlinear ion Landau damping or electron orbit perturbations are negligible. The kinetic wave equation describing the excited electron plasma wave may then be written in a WKB approximation form as (DuBois and Goldman, 1972a; Valeo, Oberman and Perkins, 1972)

$$\frac{1}{2\omega}\left(\frac{\partial}{\partial t} + \underset{\sim}{v}_g \cdot \frac{\partial}{\partial \underset{\sim}{r}}\right)\mathcal{E}_k = \left[\left(\frac{\omega_0}{\omega_p}\right)^2 \frac{\mathcal{E}_0 S\mu^2}{1+d^2} - \frac{\gamma_e}{\omega}\right]\mathcal{E}_k + \frac{\alpha k \gamma_e}{k_D \omega} + \left(\frac{\omega_0}{\omega_p}\right)^2 \frac{\mathcal{E}_0 S\mu^2}{1+d^2} , \quad (15)$$

where $\underset{\sim}{v}_g$ is the group velocity of the electron plasma waves; α is the square root of the ion electron mass ratio; k_D is the Debye wave number; μ is the direction cosine of $\underset{\sim}{k}$ with respect to the pump field $\underset{\sim}{E}_0$ which is aligned with the geomagnetic field; γ_e and γ_a are the linear damping rates of the electron plasma and ion acoustic waves, respectively, and

$$\mathcal{E}_k = \left(\frac{\alpha k}{4\pi k_D}\right)\frac{I_k}{\Theta} , \quad \mathcal{E}_0 = \frac{\epsilon_0}{16 n_0 \Theta} |E_0|^2 , \quad d = \frac{\omega_0 - \omega - \omega_a}{\gamma_a} . \quad (16)$$

We define n_0 as the electron density at the reflection height; Θ as the electron temperature in energy units, and

$$I_k = \lim_{V,T \to \infty} \frac{\int d\omega |E_k(\underset{\sim}{k},\omega)|^2}{2\pi VT} \quad (17)$$

as the spectral density of the electron plasma waves. The dispersion relations for the plasma and ion acoustic waves are given approximately by

$$\omega^2 = \omega_p^2\left[1 + 3\left(\frac{k}{k_D}\right)^2\right], \qquad \omega_a = \alpha k v_e \approx \gamma_a \ , \tag{18}$$

where v_e is the electron thermal velocity.

The first and second (bracketed) terms on the RHS of (15) describe the parametric growth due to the pump wave and the linear damping, respectively. The third term describes the thermal fluctuations, which are small compared to the Cerenkov radiation term, the last one. Hence, we neglect the third term (Valeo, Oberman and Perkins, 1972).

We now assume that the electron plasma wave has reached a constant amplitude at which the parametric growth is balanced by linear damping and energy loss due to propagation out of the interaction region. By using the expression for the group velocity

$$v_g = 3^{1/2} v_e \left[1 - \left(\frac{\omega_0}{\omega}\right)^2 z\right]^{1/2} \ , \tag{19}$$

Eq. (15) may be rewritten as

$$Q\left[\left(\frac{\omega}{\omega_0}\right)^2 - z\right]^{1/2} \frac{\partial \mathcal{E}_k}{\partial z} = (PS-1)\mathcal{E}_k + PS \ ,$$

$$P = \frac{\omega}{\gamma_e}\left(\frac{\omega_0}{\omega_p}\right)^2 \frac{\mathcal{E}_0 \mu^2}{1+d^2} \ , \qquad Q = \frac{3^{1/2} \mu' v_e \omega_0}{2\gamma_e H\omega} \ , \tag{20}$$

where the direction cosine of $\underset{\sim}{k}$ with respect to the z-axis, μ', is related to μ by

$$\mu' = \mu \cos\theta_0 - \sin\theta \sin\theta_0 \cos\varphi \ , \tag{21}$$

where θ_0 is the angle between the geomagnetic field and the vertical direction.

Since $P \sim (1+d^2)^{-1}$ in (20), the generated electron plasma wave has its peak near $\omega = \omega_0 - \omega_a$ at any height. For a given ω, numerical solution for $\mathcal{E}_k(z)$ is straightforward. The required boundary condition is $\mathcal{E}_k(0) = 0$ because no electron plasma wave can be generated at the base of the ionosphere.

IV. THE INCOHERENT SCATTER SPECTRUM

An incident diagnostic wave propagating vertically upward in the ionosphere is scattered by the enhanced electron plasma waves of (20). The scattered wave detected by the receiver should satisfy the synchronism conditions (Bekefi, 1966)

$$\omega_s = \omega_i \pm \omega \ , \quad k_s = k - k_i \begin{Bmatrix} \text{up-shifted} \\ \text{down-shifted} \end{Bmatrix} \ . \tag{22}$$

For incident and scattered waves with frequencies very high compared to the penetration frequency of the ionosphere, $\omega_{i,s}$ is related to $k_{i,s}$ by the simple dispersion relation

$$\omega_{i,s} = k_{i,s} c \ . \tag{23}$$

The loci in the ω,k-plane satisfying the synchronism conditions are obtained by eliminating $k_{i,s}$ and ω_s from (22) and (23) as

$$k = \frac{2\omega_i}{c} \pm \frac{\omega}{c} \quad \begin{Bmatrix} \text{up-shifted} \\ \text{down-shifted} \end{Bmatrix} \ . \tag{24}$$

These loci are shown by heavy lines in Figure 4. Since $\omega \ll 2\omega_i$, the last term on the RHS of (24) is usually dropped and the loci are considered as vertical lines at $k = \pm 2k_i$. However, it turns out to be an important term which causes the difference in magnitudes and shapes of up-shifted and down-shifted spectra.

Figure 4 also shows two dispersion curves of electron plasma waves with angular frequencies $\omega = \omega_0 - \omega_a$ for k given by (24). Since, as shown in (20), the electron plasma waves are enhanced most significantly near $\omega = \omega_0 - \omega_a$, these two are among the most important waves. The figure clearly shows that they belong to different heights. The dependence of the frequency of electron plasma waves on height is found from (18) and (24) as

$$z(\omega) = \left(\frac{\omega}{\omega_0}\right)^2 - \frac{12\,\omega_i(\omega_i \pm \omega_0)}{\omega_0^2}\left(\frac{v_e}{c}\right)^2 \qquad \begin{Bmatrix} \text{up-shifted} \\ \text{down-shifted} \end{Bmatrix} \ , \tag{25}$$

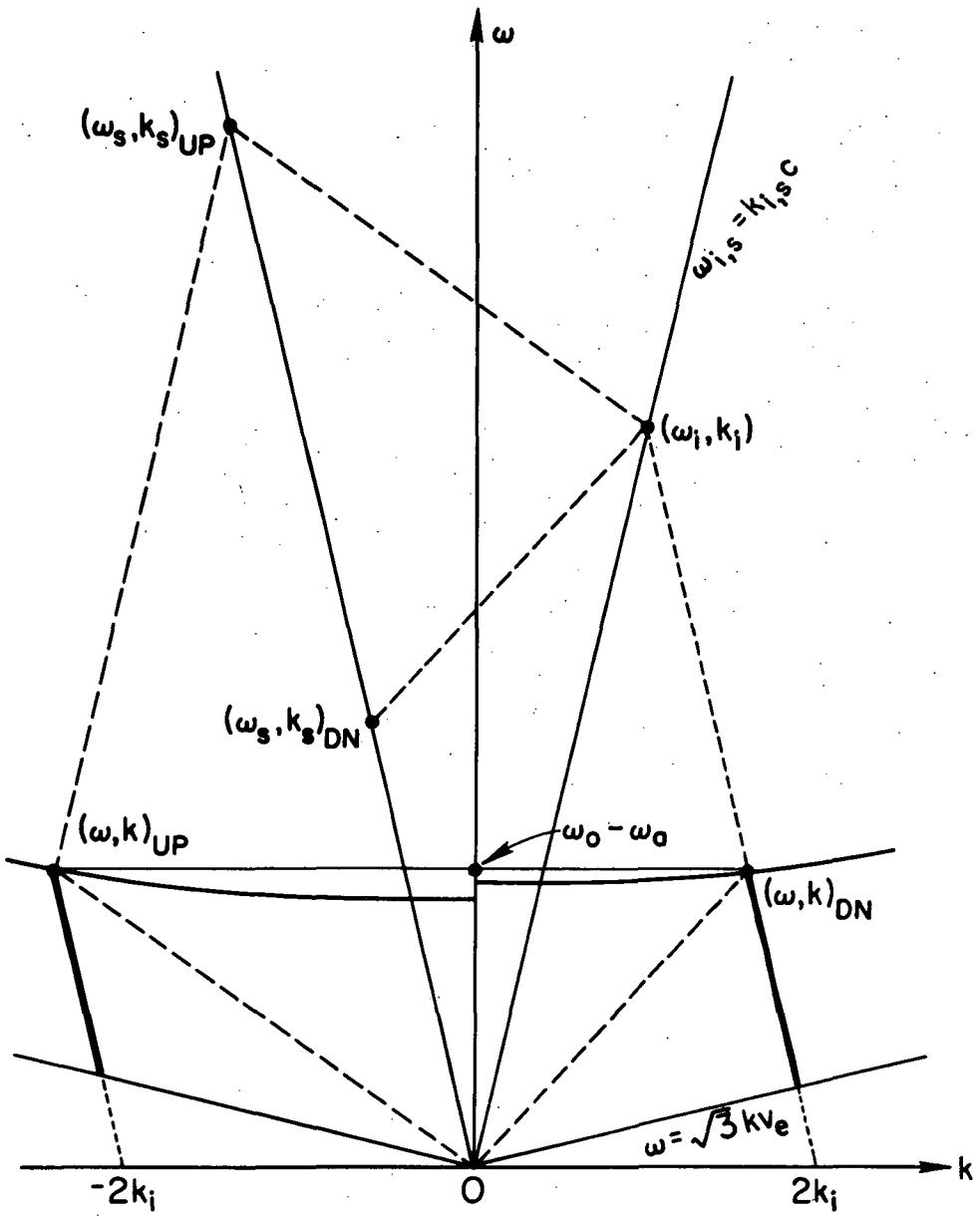

FIG. 4. The synchronism parallelogram for up- and down-shifted plasma lines.

where, since $\omega_i \gg \omega_0 \gg \omega_a$, the value of k in (24) has been taken at $\omega = \omega_0$. The heights far above two electron plasma waves are then found from (25) with $\omega = \omega_0 - \omega_a$: For typical values in the Arecibo experiment of $f_0 = 5.62$ MHz, $f_i = 430$ MHz, $f_a = 4$ kHz, $T_e = 1200^{\circ}$K and $H = 3 \times 10^4$ m, they are

$$h_M \approx H - \begin{Bmatrix} 4.75 \\ 4.64 \end{Bmatrix} \times 10^2 \text{ m}, \qquad \begin{Bmatrix} \text{up-shifted} \\ \text{down-shifted} \end{Bmatrix}. \tag{26}$$

The height where the maximum up-shifted plasma line comes from is about 10 m below that for the maximum down-shifted plasma line. The magnitudes of the swelling factor at these heights are shown in Figure 3. Consequently, different intensities of the electron plasma waves at these heights are expected from (20), which in turn result in different magnitudes of up-shifted and down-shifted spectra. The power scattered by the enhanced plasma waves is given by (Harker, 1972) as

$$dP_s = \frac{n\sigma_T}{\alpha h_o} \left(\frac{k}{k_D}\right) \frac{P_t A_r}{(z+h/h_0)^2} \mathcal{E}_k \, dz , \tag{27}$$

where A_r is the receiver aperture area; P_t is the transmitted radar power, and the Thompson backscattering cross-section, σ_T, may be taken as the square of the classical electron radius for the present purpose,

$$\sigma_T = r_0^2 = 7.94 \times 10^{-30} \text{ m}^2 . \tag{28}$$

From (25), the variable z may be changed to ω via

$$dz = 2 \frac{\omega}{\omega_0^2} d\omega . \tag{29}$$

Equation (27) then yields

$$\frac{dP_s}{d\omega} = \frac{2n_0 \sigma_T v_e P_t A_r \, (2\omega_i \pm \omega)\omega}{\alpha c h_0 \omega_0^3} \left[\frac{z^{1/2}}{(z-h/h_0)^2}\right] \mathcal{E}_k[z(\omega)] , \tag{30}$$

where n_0 is n at the reflection height. The power spectrum is plotted in Figure 5, with the phase of the reflection coefficient as a parameter, and with typical values for the Arecibo experiment:

$$T = 1200^{\circ}K \ , \quad H = 30 \text{ km} \ , \quad h = 150 \text{ km} \ ,$$

$$\begin{aligned} f_0 &= 5.62 \text{ MHz} \quad , \quad \theta_0 = 40^{\circ} \ , \\ f_a &= \gamma_a/2\pi = 4 \text{ kHz} \quad , \quad P_0 = 100 \text{ kW} \ , \\ f_e &= \gamma_e/2\pi = 650 \text{ Hz} \quad , \quad P_T = 2.5 \text{ MW} \ , \\ f_i &= 430 \text{ MHz} \quad , \quad R = 1/2 \ , \end{aligned} \tag{31}$$

Antenna diameter = 300 m , Antenna efficiency = 40% .

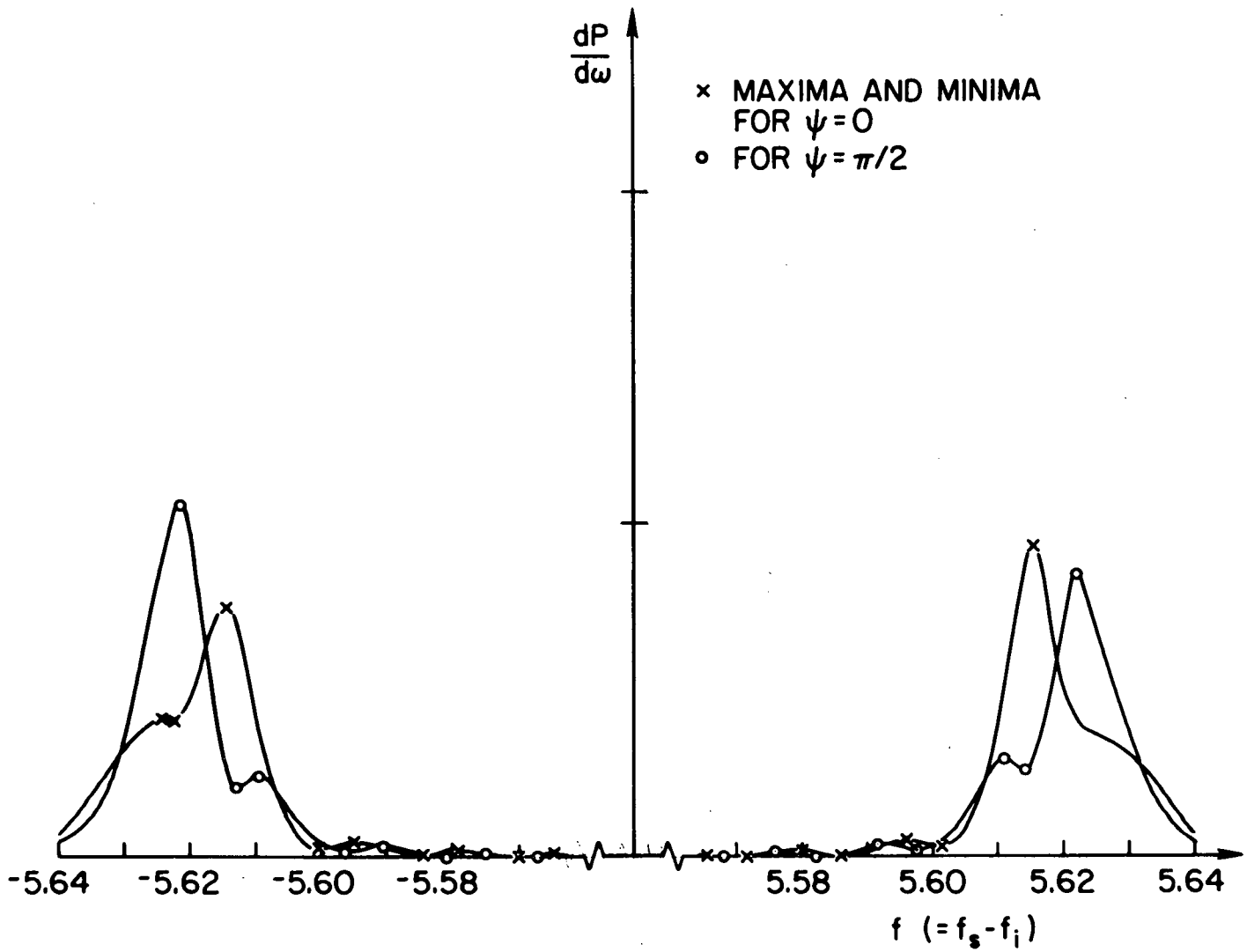

FIG. 5. Frequency spectra (a) when $\psi = 0$ and $\pi/2$.

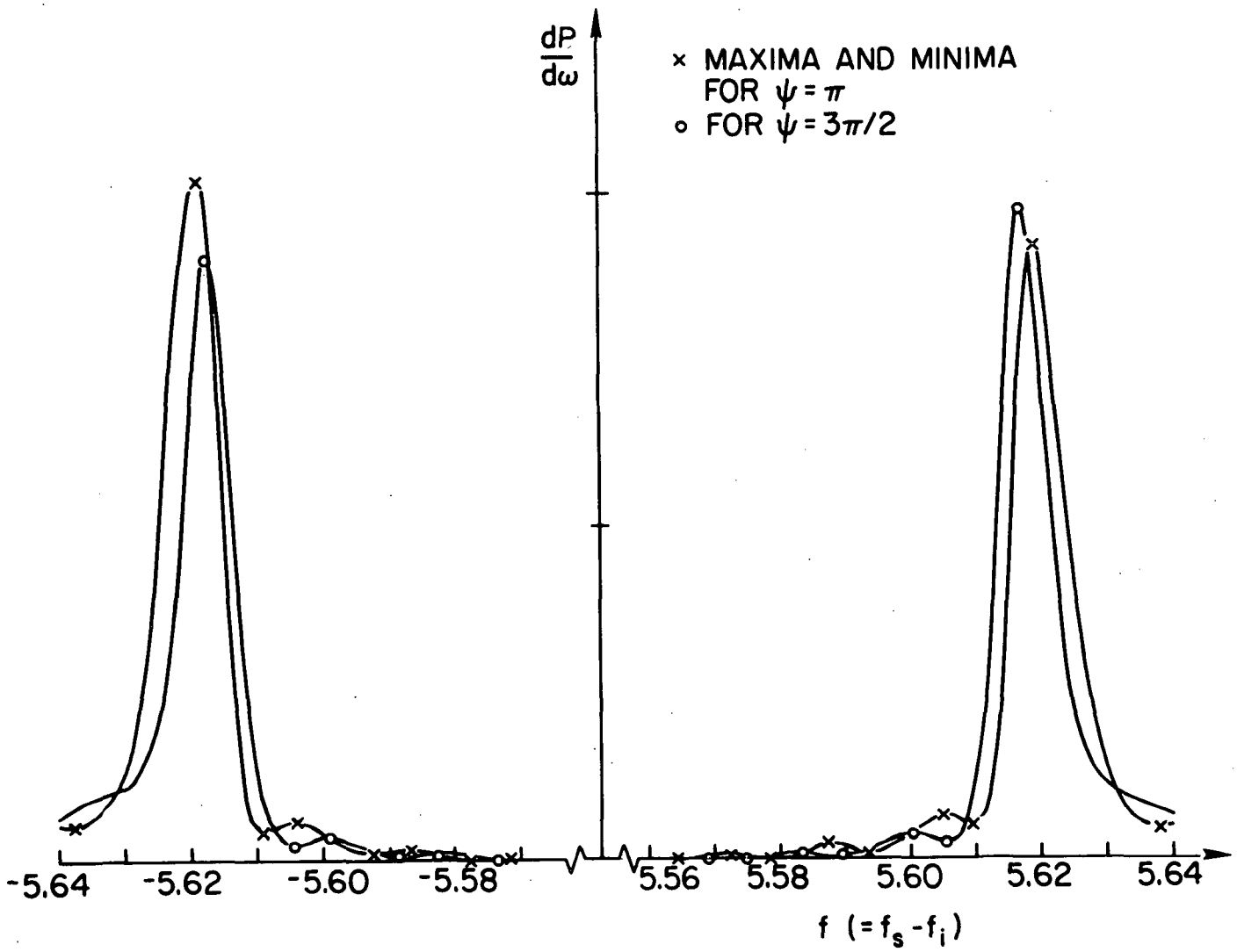

FIG. 5 (contd). (b) when $\psi = \pi$ and $3\pi/2$.

V. DISCUSSION

Our theory has been based on the subthreshold condition: in contrast to previous analyses, we have neglected nonlinear Landau damping of electron plasma waves by positive ions or effects of nonlinearly perturbed electron orbits as higher order processes. Since most of the energy deposition from the pump wave occurs at the reflection level ($z = 1$), the intensity of the enhanced electron plasma wave may be well above the instability threshold. However, as shown in (26), the strongest echo received does not come from the reflection level, but from a region about 0.5 km below for typical experimental data obtained at Arecibo. In this region, the pump power from a 100 kW radar is about 0.8 times the threshold at most. In passing, we also note that the WKB approximation we have employed is valid in this region.

Inclusion of the geomagnetic field may add to the RHS of (18) an additional term $\omega_c^2 \sin^2\theta$, where ω_c is the electron cyclotron frequency due to the geomagnetic field. Though this is larger than the thermal correction term in the dispersion relation, assuming that $\omega_c \sin\theta \ll \omega_0$, and that the spatial dependence be much weaker than that of the wave vector k, gives (20) and (25) as good approximations. Thus, the geomagnetic effect does not invalidate the present results.

For a particular phase of the reflection coefficient, each spectrum in Figure 5 has peaks near $f = \pm(f_0 - f_a)$. These are due to electron plasma waves parametrically enhanced by the pump wave. The intensities of the up-shifted and down-shifted peaks differ from each other. This is due to the difference in heights where the scattered waves of $f = \pm(f_0 - f_a)$ are generated as calculated in (26), i.e., as shown in Figure 3, there is a difference in the swelling factors at these heights. While the down-shifted peaks are smaller than the up-shifted in Figure 5 for the phases of the reflection coefficient, $\psi = 0$ and $3\pi/2$, the spectra for $\psi = \pi/2$ and π, where the down-shifted peaks are larger than the up-shifted, correspond to the experimental observations.

Consistent with the spectra obtained at Arecibo, there are several maxima and minima near the peak of each spectrum. These are due to the swelling factor. The frequency intervals between adjacent maxima (15 $\sim$ 17 kHz) are in good agreement with the experimental results (8 $\sim$ 20 kHz) (Kantor, 1972).

ACKNOWLEDGMENT

The author wishes to thank Dr. K. J. Harker and Prof. F. W. Crawford for suggesting the problem,and many helpful discussions. The work was supported by the Advanced Research Projects Agency of the Department of Defense under Contract N00014-67-A-0112-0066 monitored by the Office of Naval Research, and by the National Aeronautics and Space Administration under Grant NGL 05-020-176.

REFERENCES

Abramowitz, M., and I. A. Stegun, Handbook of Mathematical Functions, U.S. Government Printing Office, Washington, D. C., 1964.

Arnush, D., B. D. Fried, and C. F. Kennel, Propagation of parametrically generated electrostatic waves, Abstracts for Symposium on the Anomalous Absorption of Intense Radiation, Boulder, Colorado, March 1972a.

Arnush, D., B. D. Fried, and C. F. Kennel, Ionospheric propagation of electronic sidebands generated by parametric instability, Abstracts for the Spring Meeting of URSI, 1972b.

Bekefi, G., Radiation Processes in Plasmas, John Wiley and Sons, New York, 1966.

Bezzerides, B., and J. Weinstock, Nonlinear saturation of parametric instabilities, Phys. Rev. Letters, 28, 481, 1972.

Budden, K. G., Radio Waves in the Ionosphere, Cambridge University Press, Cambridge, 1961.

Carlson, H. C., W. E. Gordon, and R. L. Showen, High frequency induced enhancements of the incoherent scatter spectrum at Arecibo, J. Geophys. Res., 77, 1242, 1972.

DuBois, D. F., and M. V. Goldman, Radiation-induced instability of electron plasma oscillations, Phys. Rev. Letters, 14, 544, 1965.

DuBois, D. F., and M. V. Goldman, Nonlinear saturation of parametric instability: Basic theory and application to the ionosphere, Phys. Fluids, 15, 919, 1972a.

DuBois, D. F., and M. V. Goldman, Spectrum and anomalous resistivity for the saturated parametric instability, Phys. Rev. Letters, 28, 218, 1972b.

Fejer, J. A., and Kuo, Y-Y., Structure in the non-linear saturation spectrum of parametric instabilities, Department of Applied Physics and Information Science Rept., University of California, San Diego, California, December 1972.

Ginzburg, V. L., The Propagation of Electromagnetic Waves in Plasmas, Pergamon Press, Oxford, 1964.

Harker, K. J., J. Geophys. Res., 77, 6904, 1972.

Kantor, I. J., Plasma Waves Induced by HF Radio Waves, Ph.D. Thesis, Rice University, Houston, Texas, July 1972.

Kruer, W. L., and E. J. Valeo, Nonlinear evolution of the decay instability in a plasma with comparable electron and ion temperatures, Plasma Phys. Lab. Rept. MATT-919, Princeton University, Princeton, N. J., August 1972.

Kuo, Y-Y., and J. A. Fejer, Spectral-line structures of saturated parametric instabilities, Phys. Rev. Letters, 29, 1667, 1972.

Nishikawa, K., Parametric excitation of coupled waves I. General formulation, J. Phys. Soc. Jap., 24, 916, 1968.

Perkins, F. W., and E. J. Valeo, Parametric instabilities and ionospheric modifications, Abstracts for Symposium on the Anomalous Absorption of Intense High Frequency Waves, Los Alamos, New Mexico, March 1973.

Valeo, E., C. Oberman, and F. W. Perkins, Saturation of the decay instability for comparable electronic and ionic temperatures, Phys. Rev. Letters, 28, 340, 1972.

UNCLASSIFIED

Security Classification

DOCUMENT CONTROL DATA – R & D

(Security classification of title, body of abstract and indexing annotation must be entered when the overall report is classified)

1. ORIGINATING ACTIVITY *(Corporate author)*
Institute for Plasma Research
Stanford University
Stanford, California 94305

2a. REPORT SECURITY CLASSIFICATION
UNCLASSIFIED

2b. GROUP

3. REPORT TITLE

ANALYSIS OF THE BACKSCATTER SPECTRUM IN AN IONOSPHERIC MODIFICATION EXPERIMENT

4. DESCRIPTIVE NOTES *(Type of report and inclusive dates)*
Scientific Technical

5. AUTHOR(S) *(First name, middle initial, last name)*

Hongjin Kim

6. REPORT DATE	7a. TOTAL NO. OF PAGES	7b. NO. OF REFS
28 June 1973	25	19

8a. CONTRACT OR GRANT NO.
N00014-67-A-0112-0066

b. PROJECT NO.
ARPA Order No. 1733; Program Code 2E20

c.

d.

9a. ORIGINATOR'S REPORT NUMBER(S)
SUIPR Report No. 509

9b. OTHER REPORT NO(S) *(Any other numbers that may be assigned this report)*

10. DISTRIBUTION STATEMENT
Approved for public release; distribution unlimited.

11. SUPPLEMENTARY NOTES
Sponsored by ARPA and monitored by ONR (Code 418)

12. SPONSORING MILITARY ACTIVITY
Office of Naval Research
Field Projects Programs, Code 418
Arlington, Virginia 22217

13. ABSTRACT

The purpose of this study is to compare predictions of the backscatter spectrum, including effects of ionospheric inhomogeneity, with experimental observations of incoherent backscatter from an artificially heated region. Our calculations show that the strongest backscatter echo received is not, in fact, from the reflection level, but from a region some distance below (about 0.5 km for an experiment carried out at Arecibo), where the pump wave from a HF transmitter ($\sim$ 100 kW) is below the threshold for parameteric amplification. By taking the standing wave pattern of the pump into account properly, the present theory explains the asymmetry of the up-shifted and down-shifted plasma lines in the backscatter spectrum, and the several peaks typically observed in the region of the spectrum near the HF transmitter frequency.

DD FORM 1 NOV 65 1473

UNCLASSIFIED

Security Classification

14. KEY WORDS	LINK A		LINK B		LINK C	
	ROLE	WT	ROLE	WT	ROLE	WT
BACKSCATTER INCOHERENT SCATTER						